Flow of Magnetohydrodynamic Micropolar Fluid Induced by Radially Stretching Sheets

Tasawar Hayat[a,b], Muhammad Nawaz[a], and Awatif A. Hendi[b]

[a] Department of Mathematics, Quaid-I-Azam University 45320, Islamabad 44000, Pakistan
[b] Department of Physics, Faculty of Science, King Saud University, P. O. Box. 1846, Riyadh 11321, Saudi Arabia

Reprint requests to T. H.; E-mail: pensy_t@yahoo.com

Z. Naturforsch. **66a,** 53 – 60 (2011); received March 5, 2010 / revised June 5, 2010

We investigate the flow of a micropolar fluid between radial stretching sheets. The magnetohydrodynamic (MHD) nonlinear problem is treated using the homotopy analysis method (HAM) and the velocity profiles are predicted for the pertinent parameters. The values of skin friction and couple shear stress coefficients are obtained for various values of Reynolds number, Hartman number, and micropolar fluid parameter.

Key words: Micropolar Fluid; Radial Stretching; Homotopy Analysis Solution; Skin Friction Coefficient; Couple Stress Coefficient.

1. Introduction

It is now accepted that most of the fluids in industry and engineering are non-Newtonian in nature. Particularly, such fluids are prominent in plastic manufacture, lubrications, applications of paints, in extrusion of crude oil from petroleum products, performance of glues and inks, processing of food, movement of biological fluids etc. The classical Navier-Stokes equations do not describe the flow properties of such fluids. Mostly, these fluids have nonlinear constitutive equations. The corresponding equations of non-Newtonian fluids are very complicated in comparison to the Navier-Stokes equations. In fact, the additional rheological parameters appearing in the constitutive equations add interesting complexities in the governing equations. In general, the governing equations of non-Newtonian fluids are of higher order [1 – 3] and subtle in comparison to the Navier-Stokes equations. The rheological parameters in the constitutive equations present interesting challenges to the numerical simulists and mathematicians. In view of such difficulties and the practical and fundamental association of non-Newtonian fluids to industrial problems, several researchers [4 – 15] studied the flow of non-Newtonian fluids in various geometrical configurations.

It is now known that unlike viscous fluids, the non-Newtonian fluids cannot be explained by a single constitutive equation. Therefore many models of non-Newtonian fluids are proposed in the literature. Amongst these models there is a theory of micropolar fluids proposed by Eringen [16]. This theory shows microrotation effects as well as microinertia and has great potential to discuss the flow of colloidal fluids, liquids crystal, polymeric suspension, and animal blood. The theory of micropolar fluids is quite popular amongst the researchers, and extensive work is available in the literature by using the constitutive equations of micropolar fluids. Various applications in this direction have been presented [17 – 25]. Recently, the stretching flows have received considerable attention of the researchers. This is due to their demands in aerodynamic extrusion of plastic sheets, cooling of an infinite plate in a cooling bath, liquid film in condensation process, continuous filament extrusion from a dye, the fluid dynamic of a long thread travelling between a feed roll and wind-up roll etc. Many investigations regarding stretching flows of micropolar fluid have been discussed. For instance, Takhar et al. [25] computed a finite element solution for the flow of a micropolar fluid between two porous disks. Khedr et al. [26] studied the MHD flow of a micropolar fluid past a stretched permeable surface with heat generation or absorption. Ishak et al. [27] analyzed mixed convection stagnation point flow of a micropolar fluid towards a stretching sheet. Mohammadein and Gorla [28] discussed the heat transfer characteristics in the flow of a micropolar

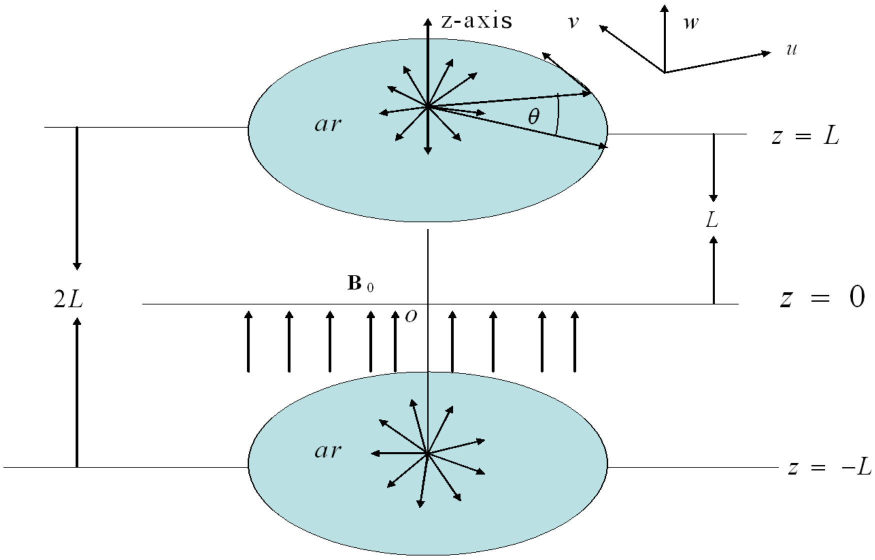

Fig. 1 (colour online). Physical model and coordinate system.

fluid over a stretching sheet with viscous dissipation and internal heat generation.

Literature survey reveals that no study regarding the flow of a micropolar fluid between two stretching sheets is available. In the present work we consider the two-dimensional flow of a micropolar fluid between two sheets. The flow is engendered due to linear radial stretching of the sheets. Analytic solution is derived by using the homotopy analysis method [29–44]. Critical assessment is made to the various pertinent flow parameters appearing in the mathematical modelling of the problem.

2. Formulation of the Problem

Let us consider the steady two-dimensional flow of an incompressible micropolar fluid between the radially stretching sheets at $z = \pm L$. We denote the velocity and microrotation components (u, v, w) and (N_1, N_2, N_3) in the cylindrical coordinates system, respectively. A constant magnetic field $\mathbf{B}_0$ is applied perpendicular to the plane of the sheets. The induced magnetic field is neglected under the assumption of small magnetic Reynolds number. No electric field is present. The physical model and the coordinate system are shown in Figure 1. The microstructure associated with spin inertia is taken into account. The relevant equations are:

$$\nabla \cdot \mathbf{V} = 0, \tag{1}$$

$$\rho \frac{\mathrm{d}\mathbf{V}}{\mathrm{d}t} = -\nabla p + (\mu + k)\nabla^2 \mathbf{V} + k\nabla \times \boldsymbol{\Omega} + \mathbf{J} \times \mathbf{B}, \tag{2}$$

$$\rho j \frac{\mathrm{d}\boldsymbol{\Omega}}{\mathrm{d}t} = (\alpha + \beta + \gamma)\nabla(\nabla \cdot \boldsymbol{\Omega}) - \gamma\nabla \times (\nabla \times \boldsymbol{\Omega}) + k\nabla \times \mathbf{V} - 2k\boldsymbol{\Omega}, \tag{3}$$

$$\mathbf{J} = \sigma[\mathbf{V} \times \mathbf{B}]. \tag{4}$$

In above equations $\mathrm{d}/\mathrm{d}t$ is the material derivative, $\mathbf{V}$ is the velocity field, $\mathbf{J}$ is the current density vector, σ is the electrical conductivity of the fluid, j is the microinertia per unit mass, $\boldsymbol{\Omega}$ is the microrotation vector, ρ is the fluid density, μ and k are the viscosity coefficients, and α, β, γ are the gyroviscosity coefficients. Furthermore, μ, k, α, β, and γ satisfy the following conditions [16]:

$$2\mu + k \geq 0, \quad k \geq 0, \quad 3\alpha + \beta + \gamma \geq 0, \quad \gamma \geq |\beta|.$$

The velocity and microrotation fields for the present problem are

$$\mathbf{V} = [u(r,z), 0, w(r,z)], \quad \boldsymbol{\Omega} = [0, N_2(r,z), 0], \tag{5}$$

where u and w are the velocity components along the radial (r) and axial (z) directions, respectively, and N_2 is the azimuthal component of the microrotation vector.

The resulting equations are given by

$$\frac{\partial u}{\partial r} + \frac{u}{r} + \frac{\partial w}{\partial z} = 0, \tag{6}$$

$$u\frac{\partial u}{\partial r}+w\frac{\partial u}{\partial z}=-\frac{1}{\rho}\frac{\partial p}{\partial r}+\frac{1}{\rho}(\mu+k)\left[\frac{\partial^2 u}{\partial r^2}+\frac{1}{r}\frac{\partial u}{\partial r}+\frac{\partial^2 u}{\partial z^2}-\frac{u}{r^2}\right]-\frac{k}{\rho}\frac{\partial N_2}{\partial z}-\frac{\sigma B_0^2}{\rho}u, \quad (7)$$

$$u\frac{\partial w}{\partial r}+w\frac{\partial w}{\partial z}=-\frac{1}{\rho}\frac{\partial p}{\partial z}+\frac{1}{\rho}(\mu+k)\left[\frac{\partial^2 w}{\partial r^2}+\frac{1}{r}\frac{\partial w}{\partial r}+\frac{\partial^2 w}{\partial z^2}\right]-\frac{k}{\rho}\left[\frac{\partial N_2}{\partial r}+\frac{N_2}{r}\right], \quad (8)$$

$$u\frac{\partial N_2}{\partial r}+w\frac{\partial N_2}{\partial z}=\frac{\gamma}{\rho j}\left[\frac{\partial^2 N_2}{\partial r^2}+\frac{1}{r}\frac{\partial N_2}{\partial r}+\frac{\partial^2 N_2}{\partial z^2}-\frac{N_2}{r^2}\right]-\frac{k}{\rho j}\left[2N_2+\frac{\partial w}{\partial r}-\frac{\partial u}{\partial z}\right], \quad (9)$$

in which $j=\nu/a$ is a reference length.

The subjected boundary conditions are

$$u=ar,\quad w=0,\quad N_2=0 \text{ at } z=L,\quad a>0,$$
$$\frac{\partial u}{\partial z}=0,\quad w=0,\quad N_2=0 \text{ at } z=0. \quad (10)$$

The arising flow equations and boundary conditions are reduced to their dimensionless form by introducing the following variables:

$$u=arf'(\eta),\quad w=-2aLf(\eta),$$
$$N_2=\frac{ar}{L}g(\eta),\quad \eta=\frac{z}{L}, \quad (11)$$

where upon our problems become

$$(1+K)f''''-\mathrm{Re}Mf''+2\mathrm{Re}ff'''-Kg''=0,$$
$$f(0)=0,\quad f(1)=0,\quad f'(1)=1,\quad f''(0)=0, \quad (12)$$

$$\left(1+\frac{K}{2}\right)g''-\mathrm{Re}K[2g-f'']+\mathrm{Re}[2fg'-f'g]=0,$$
$$g(1)=0,\quad g(0)=0, \quad (13)$$

where (6) is automatically satisfied. Here $\gamma=(\mu+k/2)j$ [24] and

$$K=\frac{k}{\mu},\quad \mathrm{Re}=\frac{aL^2}{\nu},\quad M=\frac{\sigma B_0^2}{\rho a},$$

respectively, are called the micropolar parameter, the Reynolds number, and the Hartman number.

The skin friction coefficient C_f and couple shear stress C_g at $z=L$ are defined by [25]

$$C_\mathrm{f}=\frac{\tau_w}{\rho(ar)^2}-\frac{(\mu+k)}{\rho(ar)^2}\left.\frac{\partial u}{\partial z}\right|_{z=L}=\frac{(1+K)}{\mathrm{Re_r}}f''(1),$$
$$C_\mathrm{g}=-\frac{L\gamma\left.\frac{\partial N_2}{\partial z}\right|_{z=L}}{\rho(ar)^2}=\frac{(1+K/2)}{\mathrm{Re_r}}g'(1), \quad (14)$$

where $\mathrm{Re_r}$ $(=arL/\nu)$ denotes the local Reynold number, respectively.

3. Solutions by the Homotopy Analysis Method

Here $f(\eta)$ and $g(\eta)$ are expressed by a set of base functions

$$\{\eta^{2n+1}, n\geq 0\} \quad (15)$$

in the form

$$f(\eta)=\sum_{n=0}^{\infty}a_n\eta^{2n+1}, \quad (16)$$

$$g(\eta)=\sum_{n=0}^{\infty}b_n\eta^{2n+1}, \quad (17)$$

where a_n and b_n are the coefficients. The initial guesses and linear operators L_i $(i=1,2)$ are defined by the following expressions:

$$f_0(\eta)=\frac{1}{2}(\eta^3-\eta),\quad g_0(\eta)=0, \quad (18)$$

$$L_1(f(\eta))=\frac{\mathrm{d}^4 f}{\mathrm{d}\eta^4},\quad L_2(g(\eta))=\frac{\mathrm{d}^2 g}{\mathrm{d}\eta^2}, \quad (19)$$

$$L_1[C_1+C_2\eta+C_3\eta^2+C_4\eta^3]=0, \quad (20)$$

$$L_2[C_5+C_6\eta]=0 \quad (21)$$

with C_i $(i=1-6)$ arbitrary constants. The subjected problems at the zeroth-order are given by

$$(1-q)L_1[\Phi(\eta;q)-f_0(\eta)]=q\hbar_1N_1[\Phi(\eta;q),\Psi(\eta;q)], \quad (22)$$

$$\Phi(0;q)=0,\quad \Phi(1;q)=0,$$
$$\left.\frac{\partial\Phi(\eta;q)}{\partial\eta}\right|_{\eta=1}=1,\quad \left.\frac{\partial^2\Phi(\eta;q)}{\partial\eta^2}\right|_{\eta=0}=0, \quad (23)$$

$$(1-q)L_1[\Psi(\eta;q)-g_0(\eta)]=q\hbar_2N_2[\Psi(\eta;q),\Phi(\eta;q)], \quad (24)$$

$$\Psi(1;q)=0,\quad \Psi(0;q)=0, \quad (25)$$

in which $q \in [0,1]$ and $\hbar_i \neq 0$ $(i = 1,2)$ are respectively known as the embedding and convergence control parameters such that $\Phi(\eta;0) = f_0(\eta)$, $\Psi(\eta;0) = g_0(\eta)$, $\Phi(\eta;1) = f(\eta)$ and $\Psi(\eta;1) = g(\eta)$. When q varies from 0 to 1, $\Phi(\eta;q)$ approaches from $f_0(\eta)$ to $f(\eta)$ and $\Psi(\eta;q)$ from $g_0(\eta)$ to $g(\eta)$. Furthermore, the definitions of nonlinear operators N_i $(i = 1,2)$ are

$$N_1[\Phi(\eta;q),\Psi(\eta;q)] = (1+K)\frac{\partial^4\Phi(\eta;q)}{\partial\eta^4} - \mathrm{Re}M\frac{\partial^2\Phi(\eta;q)}{\partial\eta^2} + 2\,\mathrm{Re}\,\Phi(\eta;q)\frac{\partial^3\Phi(\eta;q)}{\partial\eta^3} - K\frac{\partial^2\Psi(\eta;q)}{\partial\eta^2}, \tag{26}$$

$$N_2[\Psi(\eta;q),\Phi(\eta;q)] = \left(1+\frac{K}{2}\right)\frac{\partial^2\Psi(\eta;q)}{\partial\eta^2} - K\,\mathrm{Re}\left[2\Psi(\eta;q) - \frac{\partial^2\Phi(\eta;q)}{\partial\eta^2}\right] + \mathrm{Re}\left[2\Phi(\eta;q)\frac{\partial\Psi(\eta;q)}{\partial\eta} - \Psi(\eta;q)\frac{\partial\Phi(\eta;q)}{\partial\eta}\right]. \tag{27}$$

By using Taylor series we have

$$\Phi(\eta;q) = f_0(\eta) + \sum_{m=1}^{\infty} f_m(\eta)q^m, \tag{28}$$

$$\Psi(\eta;q) = g_0(\eta) + \sum_{m=1}^{\infty} g_m(\eta)q^m, \tag{29}$$

$$f_m(\eta) = \frac{1}{m!}\frac{\partial^m\Phi(\eta;q)}{\partial\eta^m}\bigg|_{q=0}, \tag{30}$$

$$g_m(\eta) = \frac{1}{m!}\frac{\partial^m\Psi(\eta;q)}{\partial\eta^m}\bigg|_{q=0}. \tag{31}$$

The deformation problems corresponding to the mth order are

$$\begin{aligned} &L_1[f_m(\eta) - \chi_m f_{m-1}(\eta)] = \hbar_1 R_{1m}(f_{m-1}(\eta)),\\ &f_m(0) = 0,\ f_m(1) = 0,\ f'_m(1) = 0,\ f''_m(0) = 0, \end{aligned} \tag{32}$$

$$\begin{aligned} &L_2[g_m(\eta) - \chi_m g_{m-1}(\eta)] = \hbar_2 R_{2m}(g_{m-1}(\eta)),\\ &g_m(1) = 0, \quad g_m(0) = 0, \quad \chi_m = \begin{cases} 0, & m \le 1 \\ 1, & m > 1 \end{cases}, \end{aligned} \tag{33}$$

Table 1. Convergence of HAM solutions when $\mathrm{Re} = M = 2.0$, $K = 0.5$, and $\hbar_1 = \hbar_2 = -0.7$.

Order of approximations	$f''(1)$	$g'(1)$
1	3.72000000000	−0.700000000000
5	3.61057806477	−0.738449167223
10	3.61076391320	−0.738463512754
15	3.61076396332	−0.738463496869
20	3.61076396287	−0.738463496789
25	3.61076396287	−0.738463496789
30	3.61076396287	−0.738463496789
35	3.61076396287	−0.738463496789

$$\begin{aligned} R_{1m}(f_m(\eta), g_m(\eta)) &= (1+K)f''''_{m-1} - \mathrm{Re}Mf''_{m-1} + 2\,\mathrm{Re}\sum_{n=0}^{m-1} f'''_n f_{m-1-n} - Kg''_{m-1},\\ R_{2m}(g_m(\eta), f_m(\eta)) &= \left(1+\frac{K}{2}\right)g'''_{m-1} - \mathrm{Re}\,K[2g_{m-1} - f''_{m-1}] + \mathrm{Re}\sum_{n=0}^{m-1}[2f_n g'_{m-1-n} - f'_n g_{m-1-n}]. \end{aligned} \tag{34}$$

The general solutions at the mth order are

$$f_m(\eta) = f^*_m(\eta) + C^m_1 + C^m_2\eta + C^m_3\eta^3, \tag{35}$$

$$g_m(\eta) = g^*_m(\eta) + C^m_4 + C^m_5\eta, \tag{36}$$

in which $f^*_m(\eta)$ and $g^*_m(\eta)$ are the particular solutions of (32) and (33) and the coefficients C^m_i $(i = 1-5)$ are determined by the boundary conditions given in (32) and (33). The systems (32) and (33) are solved by employing the symbolic computation program Mathematica.

4. Convergence of Homotopy Solutions

It is a known fact that the convergence of solutions given by (35) and (36) depend upon the auxiliary parameters $\hbar_1$ and $\hbar_2$. Hence, we display the $\hbar$-curves in Figures 2a and 3a. In order to show the validity of the solutions residual errors both for $f(\eta)$ and $g(\eta)$ are skeched in Figures 2b and 3b. From Figures 2 and 3 it is found that the convergence region for $f(\eta)$ and $f'(\eta)$ are $-1.15 \le \hbar_1 \le -0.4$ and that for $g(\eta)$ is $-1.1 \le \hbar_2 \le -0.6$. However, the whole analysis has been performed for $\hbar_1 = \hbar_2 = -0.7$. Furthermore, Table 1 shows that convergence is achieved at 20th-order of approximations up to 12 decimal places.

5. Results and Discussion

In order to illustrate the dimensionless velocity components and microrotation (dimensionless angular

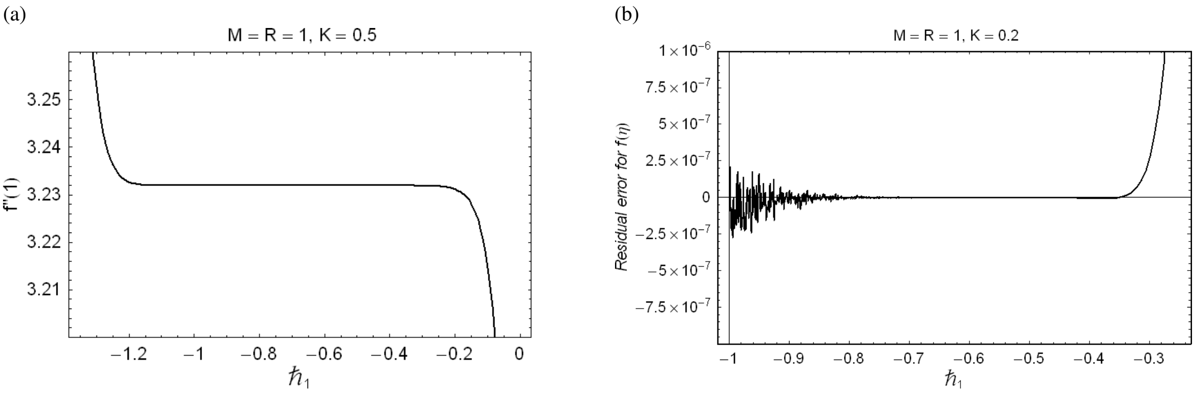

Fig. 2. (a) $\hbar$-curve of $f(\eta)$; (b) Residual error of $f(\eta)$.

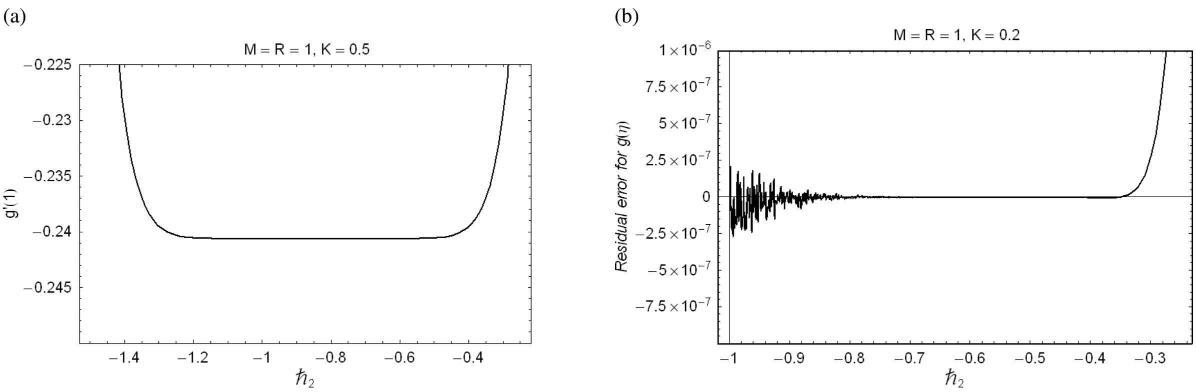

Fig. 3. (a) $\hbar$-curve of $g(\eta)$; (b) Residual error of $g(\eta)$.

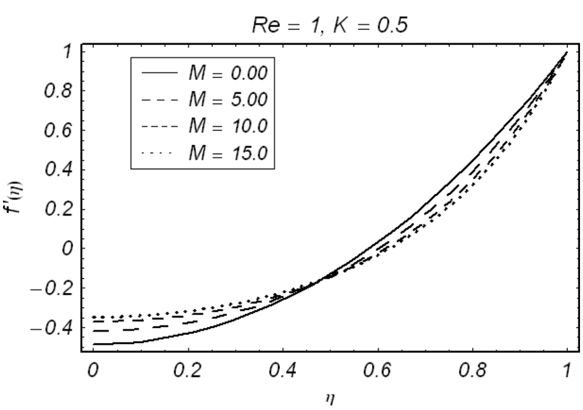

Fig. 4. Influence of M on $f'(\eta)$.

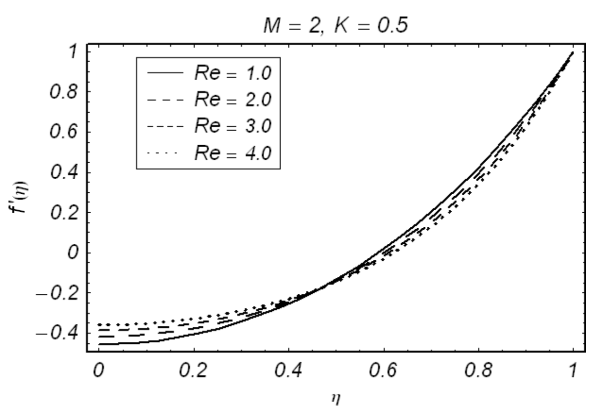

Fig. 5. Influence of Re on $f'(\eta)$.

velocity) for the emerging parameters of interest, we have plotted the Figures 4 – 12. In addition the numerical computations for skin friction coefficient and couple stress coefficient have been carried out in Table 2. It is seen from Figure 4 that the magnitude of the dimensionless radial component $f'(\eta)$ of the velocity decreases by increasing the Hartman number M. This shows that the Lorentz force retards the fluid motion in radial direction and consequently the boundary layer thickness decreases. Hence, one can conclude that the boundary layer can be controlled through the magnetic field. It is observed from Figure 5 that the magnitude

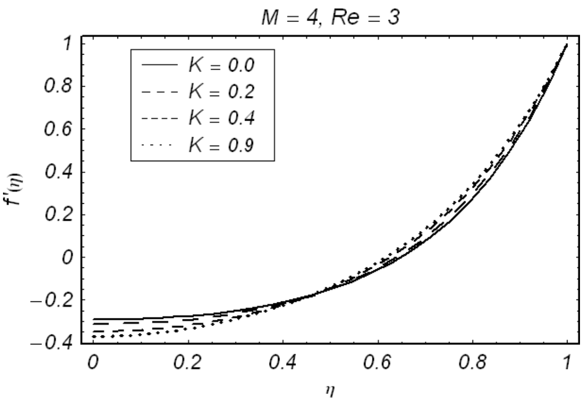

Fig. 6. Influence of K on $f'(\eta)$.

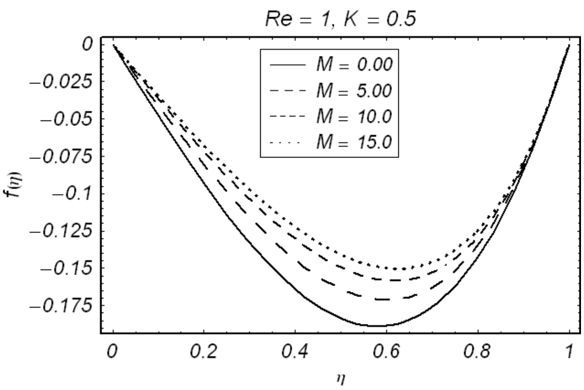

Fig. 7. Influence of M on $f(\eta)$.

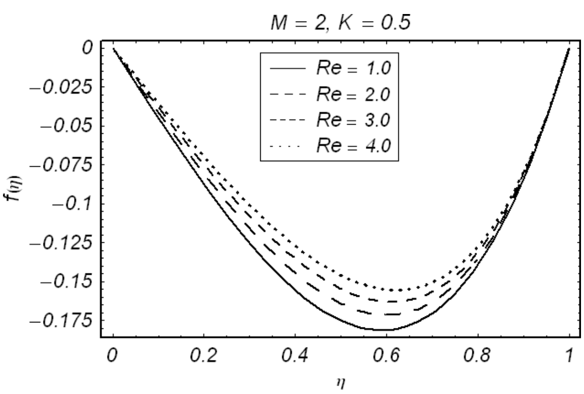

Fig. 8. Influence of Re on $f(\eta)$.

of the dimensionless radial component $f'(\eta)$ of the velocity decreases when the Reynolds number Re is increased. Upon increasing the microrotation parameter K, there is an enhancement in the magnitude of the dimensionless radial component $f'(\eta)$ of the velocity. The boundary layer thickness also increases (Fig. 6). Figure 7 depicts that the magnitude of the dimensionless axial component $f(\eta)$ of the velocity decreases for various values of Hartman number M. The influence of the Reynolds number on the dimensionless axial component $f(\eta)$ of the velocity has been shown in Figure 8. It has been found from this figure that there is a reduction in the magnitude of $f(\eta)$ when

Table 2. Numerical values of skin friction coefficient $\mathrm{Re}_\mathrm{r} C_\mathrm{f}$ and couple stress coefficient $\mathrm{Re}_\mathrm{r} C_\mathrm{g}$.

M	Re	K	$\mathrm{Re}_\mathrm{r} C_\mathrm{f}$	$-\mathrm{Re}_\mathrm{r} C_\mathrm{g}$
0.0	1.0	0.5	4.66731025187	0.918676961138
1.0			5.05533817307	0.920980526582
2.0			5.41614594430	0.923079370986
3.0			5.75398731824	0.925002385109
1.0	1.0	0.5	4.77646547374	0.478773301056
	2.0		5.05533817307	0.920980526582
	3.0		5.33415542042	1.33415055037
	4.0		5.61103357482	1.72430008392
1.0	1.0	0.0	3.31107413404	0.000000000000
		0.2	3.90500594445	0.196869286252
		0.4	4.48804832942	0.386227295205
		0.6	5.06319086907	0.570159417698

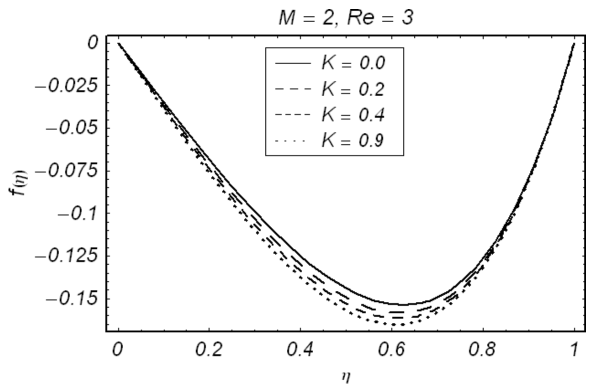

Fig. 9. Influence of K on $f(\eta)$.

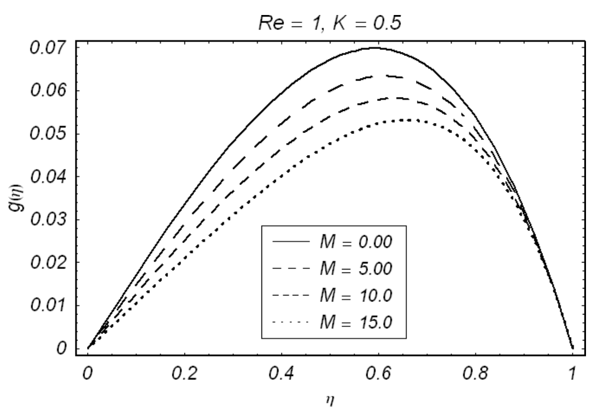

Fig. 10. Influence of M on $g(\eta)$.

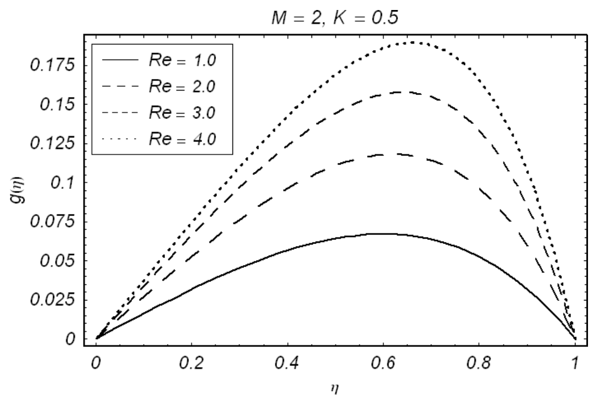

Fig. 11. Influence of Re on $g(\eta)$.

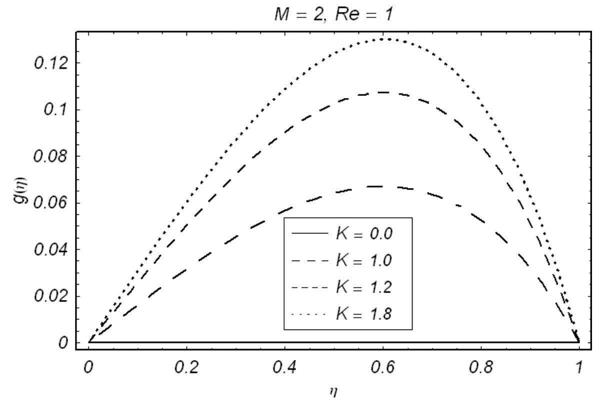

Fig. 12. Influence of K on $g(\eta)$.

Re is increased. However, the magnitude of $f(\eta)$ increases due to an increase in K (Fig. 9). The effects of M, Re, and K on the dimensionless angular velocity $g(\eta)$ are shown in Figures 10 – 12. Obviously, the dimensionless angular velocity $g(\eta)$ decreases by increasing Hartman number M as shown in Figure 10. It is also noticed that the dimensionless angular velocity $g(\eta)$ increases because of an increase in Re and K (Figs. 11 and 12). The skin friction coefficient $\mathrm{Re}_r C_f$ and the couple stress coefficient $\mathrm{Re}_r C_g$ are computed in Table 2. This demonstrates that $\mathrm{Re}_r C_f$ and $\mathrm{Re}_r C_g$ are increasing functions of M, Re, and K.

6. Concluding Remarks

A study of two-dimensional flow of an incompressible micropolar fluid between the radially stretching sheets is performed. Convergent series solution is derived through the homotopy analysis procedure. The interesting observations are presented below.

1. The velocity components $f(\eta)$ and $f'(\eta)$ are decreasing functions of Re.
2. The effect of Re on $f(\eta)$ and $g(\eta)$ are opposite.
3. There is a decrease in magnitudes of $f(\eta)$, $f'(\eta)$, and $g(\eta)$ when M is increased.
4. The applied magnetic field provides a mechanism to control the boundary layer.
5. The skin friction coefficient $\mathrm{Re}_r C_f$ and couple stress coefficient $\mathrm{Re}_r C_g$ are increasing functions of Re, M, and K.
6. Qualitative effects of M and K on the skin friction and couple stress coefficients are similar to that of Re.

Acknowledgement

We are grateful to the Higher Education Commission (HEC) of Pakistan for the financial support of this work. The useful and valuable comments of the referees are gratefully acknowledged. The first author is grateful to King Saud University for the financial support of his visit (KSU-VPP-103).

[1] K. R. Rajagopal, Acta Sin. Indica **18**, 1 (1982).
[2] K. R. Rajagopal, On the boundary conditions for fluids of the differential type, In: A. Sequira (Ed.), Navier Stokes equation and related nonlinear problems, Plenum Press, New York 1995, pp. 273 – 278.
[3] K. R. Rajagopal, A. Z. Szeri, and W. Troy, Int. J. Nonlinear Mech. **21**, 279 (1986).
[4] C. Fetecau and C. Fetecau, Int. J. Eng. Sci. **44**, 788 (2006).
[5] C. Fetecau, C. Fetecau, and D. Vieru, Acta Mech. **189**, 53 (2007).
[6] C. Fetecau, D. Vieru, and C. Fetecau, Int. J. Nonlinear Mech. **43**, 451 (2008).
[7] Z. Y. Zhang, C. J. Fu, and W. C. Tan, Phys. Fluids **20** (2008) 084103 DOI:10.1063/1.2972154.
[8] C. F. Xue, J. X. Nie, and W. C. Tan, Nonlinear Anal.: Theory, Method Appl. **69**, 2086 (2008).
[9] S. W. Wang and W. C. Tan, Phys. Lett. A **372**, 3046 (2008).
[10] C. I. Chen, C. K. Chen, and Y. T. Yang, Heat Mass Transfer **40**, 203 (2004).
[11] T. Hayat, Z. Abbas, and N. Ali, Phys. Lett. A **372**, 4698 (2008).
[12] M. Ayub, A. Rasheed, and T. Hayat, Int. J. Eng. Sci. **41**, 2091 (2003).

[13] T. Hayat, R. Ellahi, and S. Asghar, Chem. Commun. **193**, 1 (2008).
[14] T. Hayat, Z. Abbas, and T. Javed, Phys. Lett. A **372**, 637 (2008).
[15] M. Sajid, T. Hayat, S. Asghar, and K. Vajravelu, Arch. Appl. Mech. **78**, 127 (2008).
[16] A. C. Eringen, J. Math. **16**, 1 (1966).
[17] T. Ariman, M. A. Turk, and N. D. Sylvester, Int. J. Eng. Sci. **12**, 273 (1974).
[18] M. A. Ezzat, M. I. Othman, and K. A. Helmy, Can. J. Phys. **77**, 813 (1999).
[19] K. A. Helmy, H. F. Idriss, and S. E. Kassem, Can. J. Phys. **80**, 166 (2002).
[20] D. A. S. Rees and I. Pop, IMA. J. Appl. Math. **61**, 179 (1998).
[21] S. K. Jena and M. N. Mathur, Int. J. Eng. **19**, 1431 (1981).
[22] G. S. Guram and A. C. Smith, Comput. Math. Appl. **6**, 213 (1980).
[23] G. Ahmadi, Int. J. Eng. Sci. **14**, 639 (1976).
[24] R. Nazar, N. Amin, D. Filip, and I. Pop, Int. J. Nonlinear Mech. **39**, 1227 (2004).
[25] H. S. Takhar, R. Bhargava, R. S. Agrawal, and A. V. S. Balaji, Int. J. Eng. Sci. **38**, 1907 (2000).
[26] M. E. M. Khedr, A. J. Chamkha, and M. Bayomi, Nonlinear Anal.: Modelling and Control **14**, 27 (2009).
[27] A. Ishak, R. Nazar, and I. Pop, Meccanica **43**, 411 (2008).
[28] A. A. Mohammadein and R. S. R. Gorla, Int. J. Numer. Methods Heat Fluid Flow, **11**, 50 (2001).
[29] S. J. Liao, Beyond perturbation: Introduction to homotopy analysis method, Chapman and Hall, CRC Press, Boca Raton 2003.
[30] H. Xu and S. J. Liao, Commun. Nonlinear Sci. Numer. Simul. **13**, 350 (2008).
[31] S. J. Liao, Int. J. Heat Mass Transfer **48**, 2529 (2005).
[32] J. Chen and S. J. Liao, J. Math. Anal. Appl. **343**, 233 (2008).
[33] S. Abbasbandy and E. J. Parkes, Chaos, Soliton, and Fractals **36**, 581 (2008).
[34] S. Abbasbandy, Chem. Eng. J. **136**, 144 (2008).
[35] S. Abbasbandy and F. S. Zakaria, Nonlinear Dyn. **51**, 83 (2008).
[36] I. Hashim, O. Abdulaziz, and S. Momani, Commun. Nonlinear Sci. Numer. Simul. **14**, 674 (2009).
[37] A. S. Bataineh, M. S. M. Noorani, and I. Hashim, Commun. Nonlinear Sci. Numer. Simul. **14**, 409 (2009).
[38] F. M. Allan, Appl. Math. Comput. **190**, 6 (2007).
[39] T. Hayat, M. Qasim, and Z. Abbas, Z. Naturforsch. **65a**, 231 (2010).
[40] T. Hayat, M. Qasim, and Z. Abbas, Commun. Nonlinear Sci. Numer. Simul. **15**, 2375 (2010).
[41] T. Hayat, M. Mustafa, and I. Pop, Commun. Nonlinear Sci. Numer. Simul. **15**, 1183 (2010).
[42] T. Hayat and M. Nawaz, Int. J. Numer. Methods Fluids, DOI:10.1002/fld.2251.
[43] T. Hayat and M. Awais, Int. J. Numer. Methods Fluids, DOI: 10.1002/fld.2289.
[44] T. Hayat, M. Mustafa, and S. Mesloub, Z. Naturforsch. **65a**, 401 (2010).